Demonstration of InP-on-Si Self-Pulsating DFB Laser Diodes for Optical Microwave Generation

K. Ma [1,*], M. Shahin [2,3,*], *Student Member, IEEE*, A. Abbasi [2,3], *Member, IEEE*, G. Roelkens [2,3], *Member, IEEE*, and G. Morthier [2,3], *Senior Member, IEEE*

[1] *Centre for Optical and Electromagnetic Research, State Key Laboratory for Modern Optical Instrumentation, Zhejiang University, Hangzhou, China*
[2] *Photonics Research Group, Department of Information Technology (INTEC), Ghent University–IMEC, Belgium*
[3] *Center for Nano- and Biophotonics (NB-Photonics), Ghent University, Belgium*
[*] *These authors contributed equally to this work*
E-mail: Mahmoud.Shahin@UGent.be

Abstract: We demonstrate self-pulsating heterogeneously integrated III-V-on-SOI two-section distributed feedback (DFB) laser diodes, with a wide range of self-pulsation frequencies between (but not limited to) 12 and 40 GHz. The spectral width of the free-running pulsations is 40 MHz. The dependence of the self-pulsation frequency on the injected current combination and the temperature is investigated. Finally, locking the self-pulsation to an electrical RF signal with power as low as -17 dBm is demonstrated, which can be used for the generation of an optical microwave carrier with a spectral width less than 10 Hz. Such laser could be beneficial for radio-over-fiber applications.

Index Terms: Distributed Feedback Lasers, Silicon Photonics, Integrated Optics Devices, Semiconductor Lasers, Self-Pulsating Lasers, Radio-over-Fiber, Optical Microwave.

1. Introduction

Self-pulsating Distributed Feedback (DFB) laser diodes have been described in literature since the early 1990s, both single section DFB lasers [1] and two- or three-section DFB lasers [2, 3]. In single section DFB lasers, self-pulsations were mainly attributed to spatial hole burning. However, spatial hole burning has a cut-off frequency that is inversely proportional with the carrier lifetime and self-pulsation frequencies in single section DFB lasers are therefore limited to just a few GHz. In two- or three-section DFB laser diodes, self-pulsations are either due to self-Q-switching or beating-type oscillations [4]. Self-Q-switching can be based either on saturable absorption [5] or dispersive self-Q-switching [4, 6]. Self-pulsating multi-section laser diodes with saturable absorber are very much limited in frequency, but dispersive self-Q-switched DFB lasers have shown self-pulsation frequencies as high as 64 GHz [7]. Self-pulsations were studied intensively in the 1990s, e.g. due to their potential application in optical clock recovery of return-to-zero (RZ) signals in optical communication networks. Clock recovery at 40 Gb/s has been demonstrated using InP multi-section DFB lasers [8].

At present, the interest in all-optical signal processing has diminished. However, the increased importance of radio-over-fiber systems has generated a strong interest in the generation of optical microwave or millimeter wave carriers [9]. Self-pulsating DFB lasers have the advantage that their self-pulsation frequency is not fixed by the cavity length as in mode locked lasers and can generally be tuned over several GHz. Although alternative methods exist to generate optical microwave or millimeter wave carriers, e.g. direct or external laser modulation, self-pulsating laser diodes can be locked to a weak RF signal. Using this locking, an optical RF signal with very narrow linewidth could be generated with minimal RF power [10].

So far, all reported self-pulsating laser diodes were implemented as monolithic III-V laser diodes. There is, however, an increasing interest in silicon photonics and in light sources on silicon [11, 12], mainly due to the advantages of dense integration of active and passive waveguide circuits and the possibility of co-integration with electronics. Moreover, photonic integrated circuits in silicon-on-insulator (SOI) have recently gained momentum in microwave photonics applications [13].

In this paper, we report on the design, fabrication and characterization of self-pulsating heterogeneously integrated III-V-on-SOI two-section DFB laser diodes. We demonstrate their operation at high frequencies up to 40 GHz. Furthermore, we discuss on how the self-pulsation frequency can be tuned over a broad range by variation of current and temperature. Finally, we also report on the locking of the self-pulsation to a low power electrical RF signal, which can be used for the generation of optical microwave carriers with very narrow linewidth.

2. Design and Fabrication

The fabricated DFB lasers have two sections with different Bragg wavelengths. An extra phase section is often desired to allow independent control of output power and self-pulsation frequency. We have chosen to design and fabricate two-section DFB lasers (i.e. without a phase section, for simplicity). The different Bragg wavelengths are obtained via different modal effective indices, which is achieved by different widths of the InP mesa (as shown in Fig. 1) [14]. The two sections are electrically isolated by a cut through the p-InGaAs layer and part of the p-InP layer. Both sections are driven above threshold, which is the characteristic feature of beating type self-pulsations [4]. By varying the current combination into the two laser sections, the lasing wavelengths can be tuned and hence the generated self-pulsation frequency is changed.

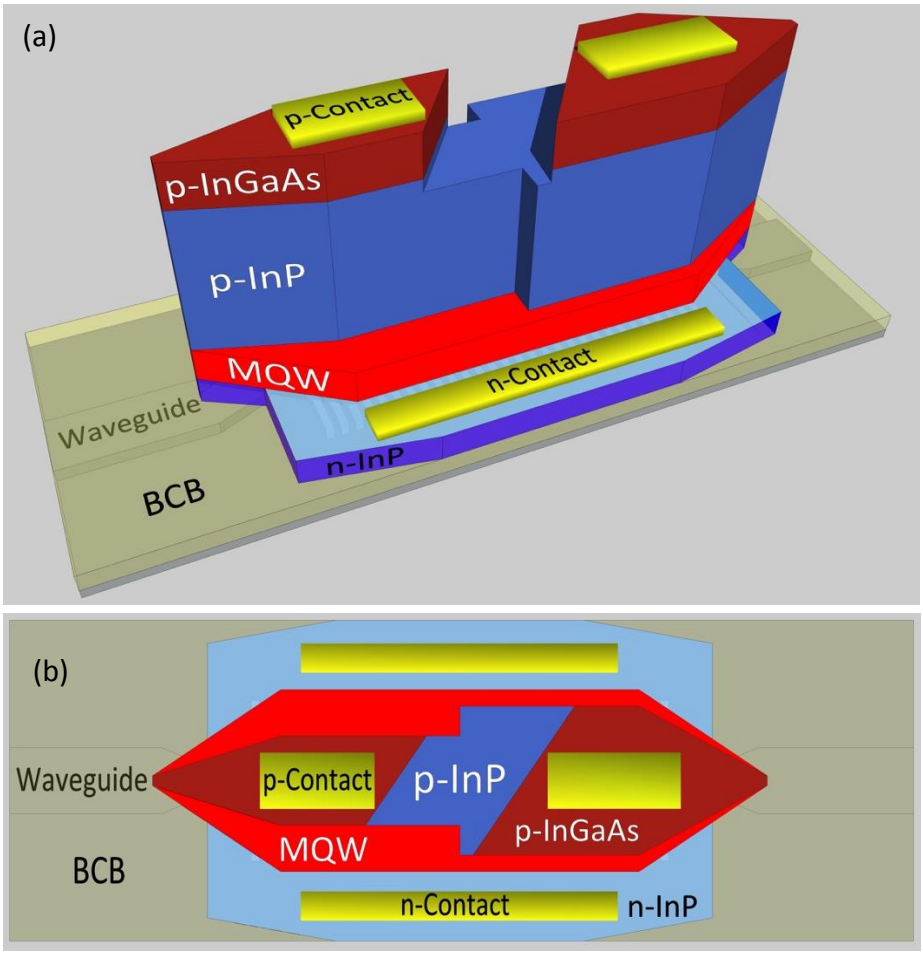

Figure 1. Schematic layout of the two-section DFB laser. (a) 3D view. (b) Top view. Different mesa widths are patterned, and an electrical isolation is made by dry etching p-InGaAs and part of the p-InP.

Many details about the fabrication of such laser diodes have been reported elsewhere [11, 12]. The fabrication starts by bonding InP-based dies comprising the laser epitaxial material onto SOI dies by adhesive bonding using DVS-BCB (divinylsiloxane-bis-benzocyclobutene). The bonding reaches close to 100% bonding yield. Coupling between the InP waveguide and the 400 nm thick silicon waveguide is realized by means of adiabatic tapers (as described in [11]), while coupling from the silicon waveguide to optical fiber occurs by means of surface grating couplers. By largely removing the planarizing oxide on top of the silicon, a very thin bonding layer of around 10 nm is obtained, as shown in Fig. 2. The misalignment of around 200 nm between the III-V waveguide layer and the silicon device layer has a negligible impact on the coupling efficiency.

The III-V epitaxial stack consists of a 190-nm-thick n-InP cladding, an active layer consisting of six 7-nm-thick InGaAsP quantum-well layers and seven 9-nm-thick InGaAsP barriers surrounded by two 100-nm-

thick separate confinement InGaAsP layers, a 1500-nm-thick p-InP cladding and a 200-nm-thick p-InGaAs contact layer. A mesa is etched down to the n-InP cladding layer (i.e. n-contact layer). A 9-μm-wide quantum-well layer is used to reduce surface recombination. The mesa width is different in both sections and has a value of 4 μm in the right section and 2 μm (Laser A) or 2.5 μm (Laser B) in the left section. Each section has a length of 480 μm (220-μm-long pumped taper included). The grating defined in the silicon waveguide layer is etched 180 nm and has a period of 240 nm (duty cycle 50%). From the width of the stop-band observed in the optical spectra, a coupling coefficient of around 150 cm^{-1} could be derived [12]. Fig. 3 shows a top view during device fabrication, in which the transition between the 2 and 4 μm wide mesas and the electrical isolation are visible.

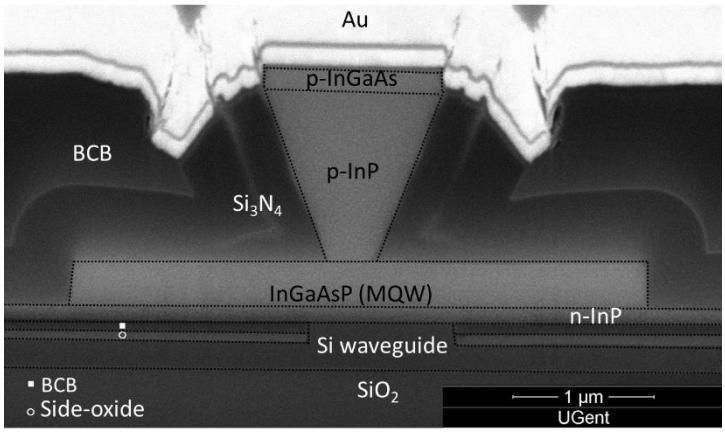

Figure 2. FIB cross-section of the fabricated devices (close to the III-V taper tip). After bonding, the mesa is etched, followed by passivation by Si_3N_4 and BCB, and finally metallization.

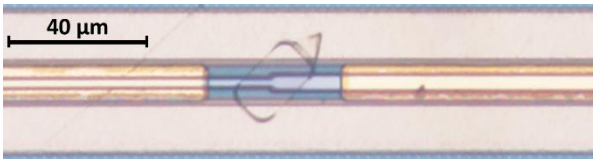

Figure 3. Top-view showing the electrical isolation and the mesa width transition.

3. Characterization

The lasers demonstrated a threshold current of 2 × 12 mA (i.e. 12 mA in each section). Fig. 4 shows the output power coupled from the left grating coupler vs. the current in the left or right laser section for laser B (laser A shows a similar trend). The current into the other section is fixed at 0, 10 and 50 mA.

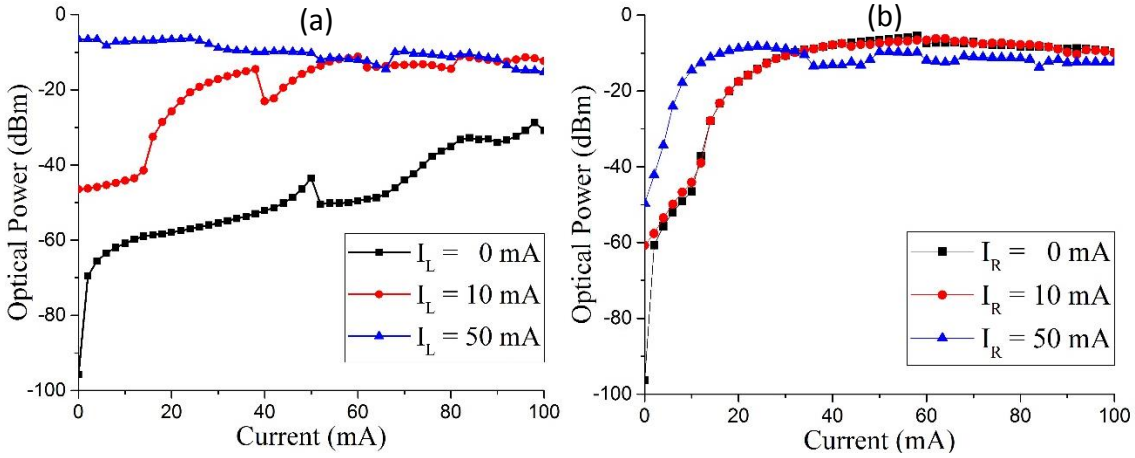

Figure 4. Output power in fiber as a function of the current into the right section (a) and into the left section (b) for Laser B. The current into the other section was fixed at 0, 10 and 50 mA.

The illustrated power curve corresponds to power measurements in the fiber and it includes the grating coupler losses. The loss caused by the grating coupler is around 8 dB near 1550 nm. When the current in the left (right) section is low, the lasing is mainly determined by the right (left) section, with the left (right) section operating as travelling wave optical amplifier for the laser light. The stop bands of both sections don't overlap in this case and the left (right) section doesn't operate as reflector for the laser light. When both currents are high, the stop bands of both sections overlap and the lasing is more complex and determined by both sections. This can also be seen in the optical spectra. The series resistance is around 10 Ω, slightly lower (9 Ω) for the wider right section and slightly larger (11 Ω) for the narrower left section.

The optical spectra of laser B are shown in Fig. 5 for two different current combinations: (1) I_L = 32 mA / I_R = 50 mA and (2) I_L = 32 mA / I_R = 35 mA. At current combination (1), the wavelength difference between the two middle lasing modes corresponds to a 110 GHz self-pulsation frequency, which is challenging to measure. When the current of the right section is reduced to 35 mA, the wavelength difference is 0.31 nm, corresponding to a beat frequency of 38.75 GHz. A self-pulsation with this frequency is obtained and further discussed in the next section.

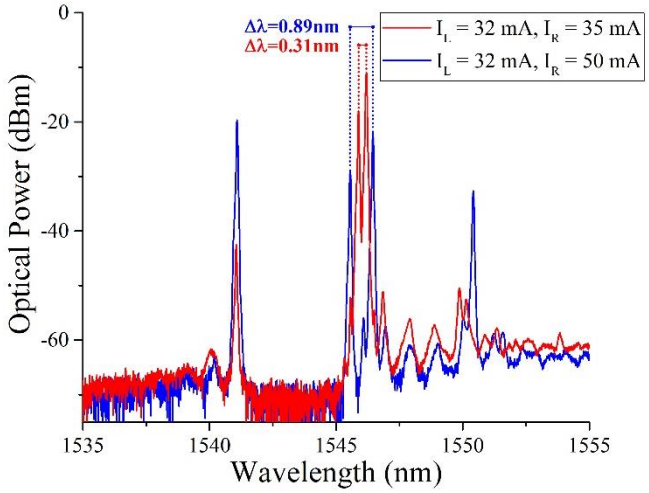

Figure 5. The optical spectrum for two bias current combinations is shown for Laser B. Depending on the combination, the distance between the peaks changes. This tunes the self-pulsation frequency.

4. Self-Pulsation Characteristics

In this section, the self-pulsation behavior of the lasers is described. The measurement setup used in this demonstration is depicted in Fig. 6. One laser section is DC biased, while the other section is supplied with a DC bias current and an RF voltage. The RF signal is injected into the right section in this measurement and similar results can be achieved when the RF signal is applied to the left section. The output is fed to an erbium-doped fiber optical amplifier (EDFA) which raises the average optical power to 0 dBm. We first investigated the characteristics of the unlocked self-pulsations, i.e. without an RF signal applied.

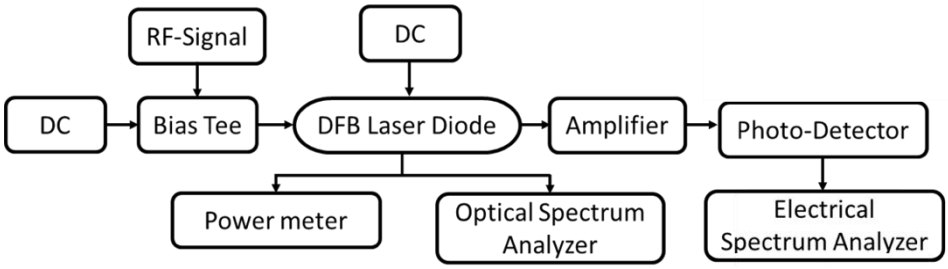

Figure 6. Block diagram of the measurement setup used in the self-pulsation characterization.

The dependence of the self-pulsation frequency on current and temperature is investigated. Fig. 7(b) gives the frequency measured when varying the current in the right section while keeping the current in the left section constant in laser A. As can be observed, the self-pulsation frequency increases with the current in the

right section. Tuning the frequency by changing the current is done over a range of 25 GHz. The opposite trend is shown in Fig. 7(a) for the left section. However, not all of the measured lasers showed the same behavior. Fig. 7(c-d) shows the current scan for laser B, in which the self-pulsation frequency decreases first and increases again as the scan current increases. This measurement was done while maintaining the substrate temperature at 15 °C. The variation of the self-pulsation frequency with currents is due to a shifting of the Bragg wavelengths in both sections. This is first of all caused by temperature increases due to Joule heating. However, since the active layer consists of strained layer multiple quantum wells, there might also be a significant influence of carrier density changes in both sections, a.o. due to the so-called gain-lever effect [15]. In laser A, the thermal effect seems to be dominant. Increasing the current in the left section e.g. causes the Bragg wavelength of that section to increase. Since that section has the lowest Bragg wavelength, an increase of it will bring both Bragg wavelengths closer and will result in a decrease of the self-pulsation frequency. In laser B, the currents in both sections are much more similar and perhaps changes in the current of one section can change the carrier distribution much more than in laser A. It can be remarked that the change of frequency with current in laser B changes direction just when the currents in both sections are about equal.

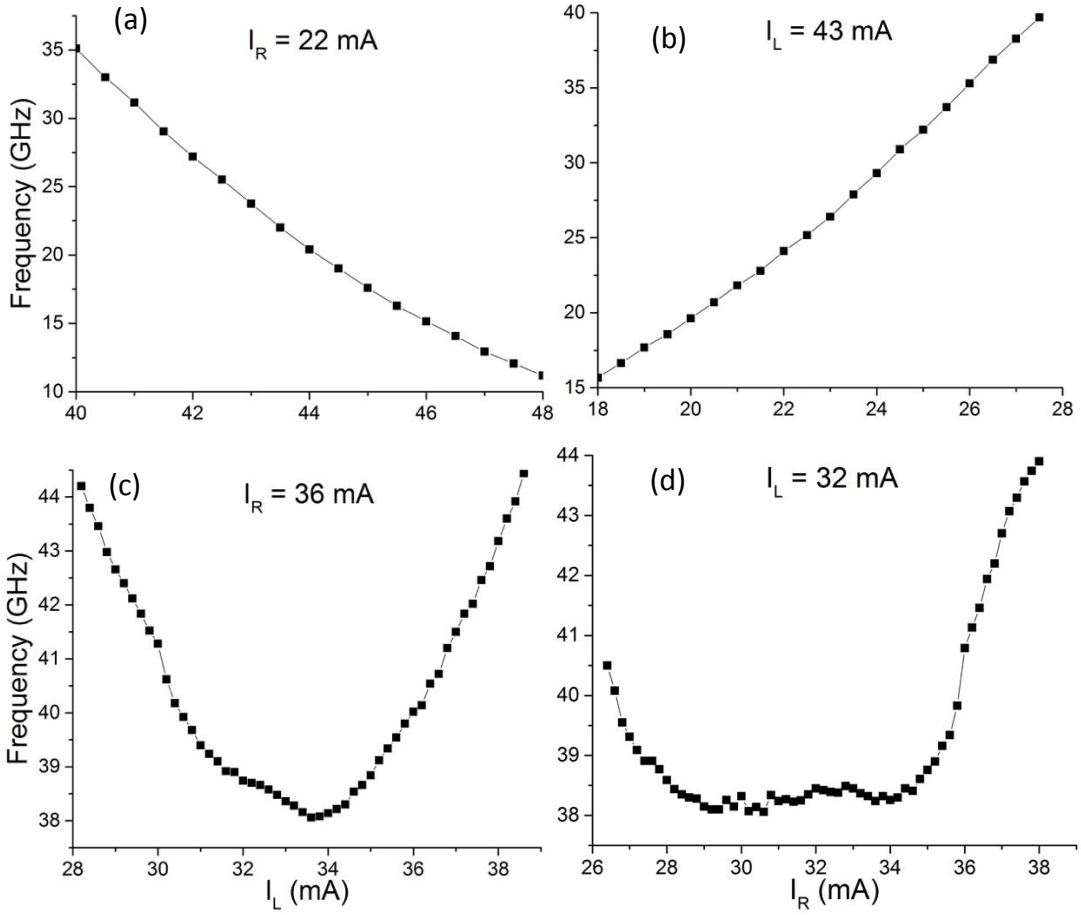

Figure 7. Variation of the self-pulsation frequency with current for laser A (a, b) and laser B (c, d).

The self-pulsation frequency is also tunable via the temperature. The temperature of the sample holder (which is assumed to be equal to the substrate temperature) was used to tune the self-pulsation frequency over a 7 GHz range. The dependence of the self-pulsation frequency on the sample holder temperature is shown in Fig. 8, in which a frequency tuning from 35 to 42 GHz can be observed for laser B.

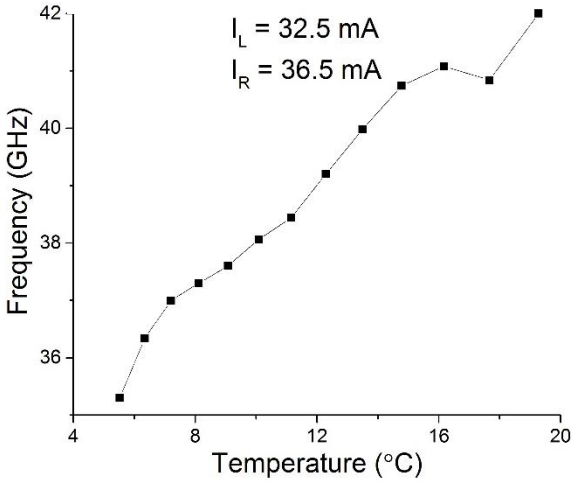

Figure 8. Tuning the substrate temperature changes the pulsation frequency over a 7 GHz range.

5. Locking the self-pulsations to an RF signal

The self-pulsation peak is shown in Fig. 9 (a). The spectral width is 40 MHz. Initially, the self-pulsation peak is not stable, and can fluctuate over few 100 MHz due to fluctuations in current and/or temperature. By applying an RF signal of -7 dBm to the laser, the spectral width was reduced significantly to below 10 Hz (Fig.9 (c)). When directly modulating the laser very close to the self-pulsation frequency, but outside of the locking range, one gets about 7 dB less RF output power, as can be seen in Figure 9. This RF output decreases further away from the self-pulsation frequency. The RF output at very high frequencies can also be expected to decrease when the laser is not self-pulsating and the modulation response has a weaker or no resonance anymore around the original self-pulsation frequency. For the signal to be locked, it should be within a range of around 300 MHz around the natural self-pulsation frequency. Increasing the RF power widens the locking range. The minimum RF power applied to the laser to generate a stable locked signal with linewidth below 10 Hz is -17 dBm, orders of magnitude lower than the 2 dBm reported in [10].

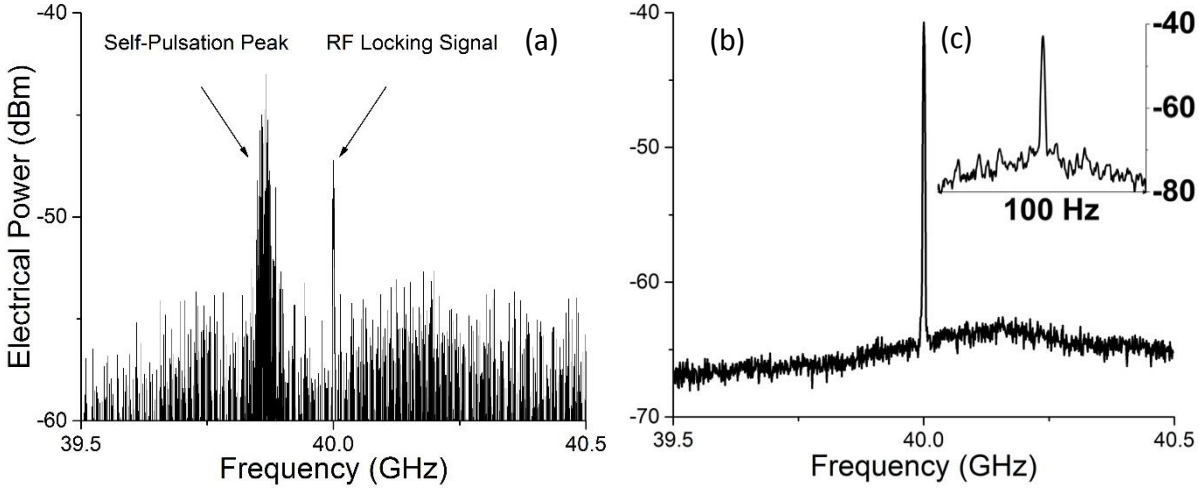

Figure 9. The self-pulsation with a spectral width of 40 MHz is shown in (a) along with a locking RF signal of -7 dBm at 40 GHz. A locked self-pulsation is shown in (b) with a spectral width of below 10 Hz in (c).

6. Conclusions

We have reported on two-section self-pulsating DFB lasers, implemented on a III-V-on-silicon integration platform. We have shown that by varying the currents and the temperature, self-pulsations can be tuned over a wide range of frequencies between (but not limited to) 12 – 40 GHz. The self-pulsations can be locked to an RF signal with a minimum power of -17 dBm, resulting in a narrow RF spectral width of less than 10 Hz. This is useful, for instance, in the generation of an optical microwave carrier, which is desired for radio-over-fiber applications.

Acknowledgement

The authors would like to acknowledge the funding of the Methusalem program of the Flemish Government. The authors also acknowledge Liesbet Van Landschoot for the FIB picture, and Michael Vanslembrouck for assisting with the measurements. Keqi Ma acknowledges the funding for doctoral students to carry out international cooperation research and the exchange program of Zhejiang University.

References

[1]. R. Schatz, "Longitudinal Spatial Instability in Symmetric Semiconductor Lasers due to Spatial Hole Burning," IEEE JQE, 28(6), pp. 1443-1449, (1992).
[2]. M. Mohrle et al., "Gigahertz self-pulsation in 1.5 μm wavelength multisection DFB lasers," IEEE PTL, 4(9), pp. 976-979, (1992).
[3]. B. Sartorius et al., "Wavelength and polarisation independent all optical synchronisation of high frequency DFB type self-pulsations," Electronic Letters, 32(11), pp. 1026-1028, (1996).
[4]. B. Sartorius et al., "Dispersive self Q-switching in self-pulsating DFB lasers," IEEE JQE, 33(2), pp. 211-218, (1997).
[5]. P. Barsnley et al., "All-Optical Clock Recovery from 5 Gb/s RZ Data Using a Self-Pulsating 1.56 prn Laser Diode," IEEE PTL, 3(10), pp. 942- 945, (1991).
[6]. M. Mohrle et al., "Detuned Grating Multisection-RW-DFB Lasers for High-Speed Optical Signal Processing," IEEE JSTQE, 7(2), pp. 217-223, (2001).
[7]. B. Sartorius et al., "All-optical clock recovery module based on self-pulsating DFB laser," Electronics letters, 34(17), pp. 1664-1665, (1998).
[8]. C. Bornholdt et al., "Self-pulsating DFB laser for all-optical clock recovery at 40Gbit/s," Electronic Letters, 36(4), pp. 327-328 (2000).
[9]. X. Qi et al., "Photonic Microwave Applications of the Dynamics of Semiconductor Lasers," IEEE JSTQE, 17(2), pp. 1198-1211, (2011).
[10]. W. Wei et al., "Realizing 60 GHz narrow-linewidth photonic microwaves with very low RF driving power," Laser Physics Letters, 13(12), pp. 126202, (2016).
[11]. S. Keyvaninia et al., "Heterogeneously integrated III-V/silicon distributed feedback lasers," Optics Letters, 38(24), pp. 5434-5437, (2013).
[12]. A. Abbasi et al., "High Speed Direct Modulation of a Heterogeneously Integrated InP/SOI DFB Laser," JLT, 34(8), pp. 1683-1687, (2016).
[13]. J. Capmany et al., "Microwave photonics: the programmable processor," Nature Photonics, 10(1), pp. 6-8, (2016).
[14]. D. Chen et al., "Self-pulsation in a two-section DFB laser with varied ridge width," Semiconductor Science and Technology, 23(1), pp. 015008 (2008).
[15]. K. Vahala et al., "The optical gain lever: A novel gain mechanism in the direct modulation of quantum well semiconductor lasers," Applied Physics Letters, 54 (25), pp. 2506-2508 (1989).